EFFECT OF SURFACE MODIFICATION BY NITROGEN-CONTAINING CHEMICALS ON MORPHOLOGY AND SURFACE CHARACTERISTICS OF N-DOPED PINE BARK BIOCHARS

Nitesh Kasera, Steven Hall, Praveen Kolar

Department of Biological and Agricultural Engineering, North Carolina State University, 3100 Faucette Drive, Raleigh, NC 27695, USA

Highlights

- Nitrogen-doped biochars have applications in environmental and energy storage.
- Melamine, urea, ammonium chloride, and ammonium nitrate were used as precursors for nitrogen doping of biochars.
- Under identical preparation conditions, melamine-doped biochar had the highest nitrogen content.
- Melamine-doped biochar exhibited the highest percentage of pyrrolic-N and pyridinic-N.
- Urea-doped biochar contained the highest percentage of graphitic-N.

Abstract. *In this study, pine bark-derived biochar was modified with melamine, urea, ammonium chloride, and ammonium nitrate to synthesize nitrogen-doped biochars. The effect of chemical modification on the extent of N-doping and surface properties were investigated. The elemental analysis suggested that melamine modified biochar samples had 4.75% nitrogen, higher than nitrogen in other modified biochars. The surface morphology and surface profile were studied with scanning electron microscopy and confocal laser scanning microscopy. X-ray photoelectron spectra showed that N-doped samples' surface nitrogen content increased to 8.3%, 3.9%, 2.3%, and 2.9% for melamine, ammonium chloride, ammonium nitrate, and urea, respectively. X-ray photoelectron spectroscopy results also revealed that among the nitrogen fractions in the N-doped biochars, melamine modified biochar has the highest percentage of pyrrolic and pyridinic nitrogen (35.2% and 36.8%, respectively) compared to others. Urea modified biochar had the highest percentage of graphitic nitrogen (26.6%). Our results suggest that application-specific nitrogen-enriched biochar can be prepared by understanding how different nitrogen precursors interact with carbon surfaces.*

Keywords. *Biochars; Nitrogen Doping; Adsorbents; Waste management; Melamine*

INTRODUCTION

Biochar has recently attracted the scientific community's attention as a substrate for the synthesis of functional carbon materials, having potential applications in energy storage technology, catalysis, wastewater treatment, and as a soil amendment (Ahmad et al., 2014; El-Naggar et al., 2018; W. J. Liu et al., 2019). Biochar is obtained by slow pyrolysis of lignocellulosic biomass (agricultural wastes, sludge, food wastes, and others). Other carbon materials – e.g., activated carbon, carbon nanotubes/nanofibers, and graphene – often require multistep preparation processes and sophisticated instruments (W. J. Liu et al., 2015). Thus, developing functional materials from biochar poses a win-win solution as it does not require sophisticated instruments which cuts down initial costs and value-added commodities can be produced economically out of wastes.

Pristine biochar obtained directly from pyrolysis exhibits poor surface functionality, low porosity, and surface area. These disadvantages limit the broad applications of biochar. However, surface functionalities and porosity of pristine biochars can be modified to improve its physicochemical properties (W. J. Liu et al., 2015). Physical activation of biochar via steam and CO_2 can improve the surface area and pore structure (Lehmann & Joseph, 2012; Xiong et al., 2013). Metal salt and metal oxide-modified biochar exhibited enhanced catalysis and adsorptive performances for degradation of trichloroethylene and mitigation of phosphorus from water, respectively (F. Liu et al., 2015; Yan et al., 2015). Modification of biochar with acid (nitric acid, sulfuric acid, oxalic acid, and others), alkali (potassium hydroxide, sodium hydroxide), and other oxidizing agents (hydrogen peroxide, potassium permanganate) increased surface oxygen functional groups (Demir et al., 2018). In addition to oxygen functional groups, nitrogen on the biochar surface can also enhance its surface reactivity by introducing active sites (Wang & Wang, 2019). Nitrogen incorporation onto biochar results in improved capacitive performance and wettability when employed as electrodes for supercapacitor applications (Demir et al., 2018; Xu et al., 2018). Moreover, doped-nitrogen can enhance biochar's overall electrochemical performance by modifying its spin and electronic characteristics (Wan et al., 2020).

Nitrogen-enriched biochars can be achieved either via *the* pyrolysis of nitrogen-rich biomasses or by modifying the biochar surfaces with nitrogen containing chemicals such as such as ammonia lithium nitrate, aniline, urea, melamine (Leng et al., 2019). These modifications alter biochars' surface chemical composition by incorporating nitrogen functional groups in the form of pyridinic-N, pyrrolic-N, amine-N, graphitic-N, amide-N, nitrile-N, and others (Zhang et al., 2017). Pyridinic-N and pyrrolic-N can donate the lone-pair electrons to participate in redox reactions and have been proven instrumental in the catalysis of oxygen reduction (Leng et al., 2019; Wan et al., 2020). Zhang et al. (2017) reported that primary and secondary amide, amines, and azo groups (N=N) on the biochar's surface could enhance CO_2 adsorption on biochar. Similarly, Shao et al. (2018) ascribed improved SO_2 removal to the presence of quaternary-N on the surface of biochar. Deng et al. (2017) reported that N-C=O groups on biochar formed metal complexes aiding the removal of heavy metals from solution. Thus, N-doped biochars based on specific end applications can be potentially produced. However, the concentration of nitrogen and the speciation of nitrogen functional groups after doping the biochar vary widely in the literature (Leng et al., 2019; Wan et al., 2020). These variations are mostly because of the inherent differences in the feedstocks employed to produce the biochars and the differences in the processing conditions.

From a material processing perspective, it is important to determine the suitability and choice of nitrogen precursor based on the target nitrogen functional groups on the biochar surfaces that might be needed for a specific application. Although the effect of different processing conditions on nitrogen functional groups of biochar had been studied, there is a dearth of knowledge of how the difference in nitrogen precursors affects biochar's nitrogen concentration and speciation. Therefore, the overarching objective of this research is to investigate the effects of different nitrogen modifying agents on the morphology and surface chemical characteristics of N-doped pine bark derived biochars.

Considering the pinewood industry's economic importance in the southeastern United States, we employed pine bark chips as a precursor material to be converted into biochar. The biochar was subsequently modified and doped with equal amounts of nitrogen from melamine, urea, ammonium chloride, and ammonium nitrate. The resultant N-doped biochars were characterized to study the differences in the biochars' morphologies and surface chemistries.

MATERIALS AND METHODS

Pine bark nuggets (6.70 ± 2.51 cm in length) were obtained locally from Oldcastle Lawn and Garden Inc., GA. The nuggets were used without any modification. All chemicals used to prepare and to characterize samples were of analytical grade. Melamine (99%, code: 125350010) and ammonium chloride (99%, code: 396400010) were obtained from Acros Organics while ammonium nitrate (≥ 99%, batch: MKBC7339) was purchased from Sigma-Aldrich. Urea (BP169-500) was procured from Fisher Scientific, USA.

SAMPLE PREPARATION

Pristine biochar samples were prepared by pyrolyzing pine bark nuggets in a box furnace (Sentry 2.0 microprocessor) at a heating rate of 10 °C min^{-1} under N_2 flow (5 L min^{-1}) up to 400 °C and maintained for 4 hours. The obtained biochar was ground and sieved to a particle size below a mesh size of 200. The samples were stored in a sealed glass container and labeled as BC. Figure 1 shows a schematic flow diagram of the different processing steps involved in the sample preparation.

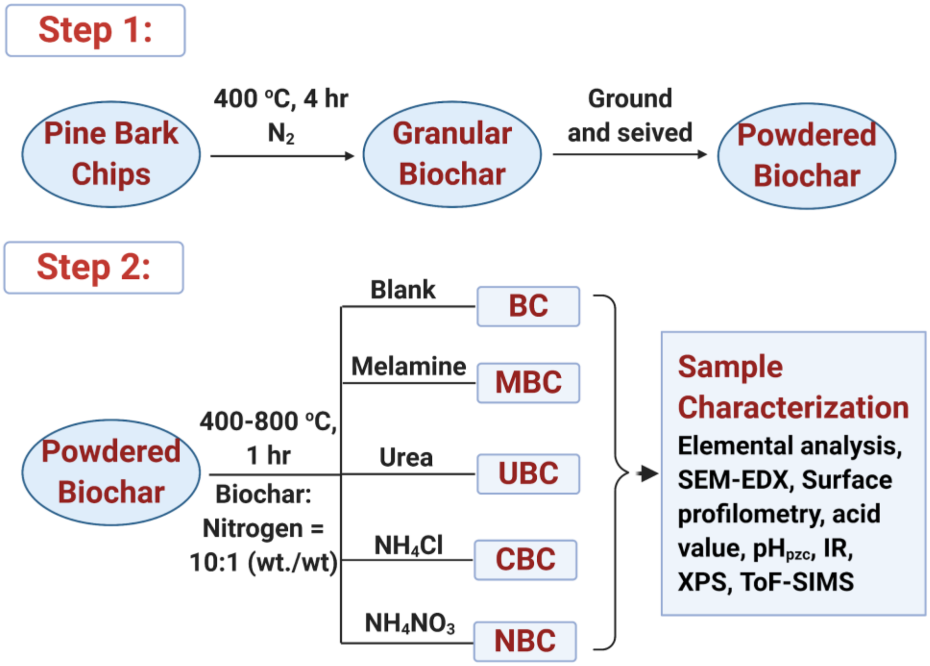

Figure 1: Schematic flow diagram showing the processing steps and characterization techniques used for different BCs (created with Biorender.com).

To prepare nitrogen modified biochar samples, 10 g of BC was mixed with 1 g nitrogen, obtained from either melamine (M), urea (U), ammonium chloride (C), or ammonium nitrate (N), in 50 mL deionized water. Respective calculations are shown in the supplementary information. In a muffle furnace (Barnstead Thermolyne 48000 Furnace; Model 48015), the obtained slurry was placed for 1 hour, after attaining the target temperature (400-800 ºC), to allow the reaction between biochar and the corresponding nitrogen containing chemicals. No gas flow was provided in this step. Subsequently, the obtained black powders were washed with 100 mL deionized water several times until the pH (pH probe - Model: AB150; Manufactured by Fisher Scientific, Waltham MA, USA) of the filtrate became neutral. The washed biochar samples were dried overnight at 105 ºC. The modified BC samples were designated as MBC, UBC, CBC, NBC-X, where X denotes the heating temperature of BC and corresponding nitrogen-containing chemical.

SAMPLE CHARACTERIZATION

A Leco CN analyzer was used to determine the elemental contents (C and N) in the BC samples. The samples' surface elemental composition was analyzed by X-ray photoelectron spectroscopy (XPS) in a SPECS XPS system with a PHOIBOS 150 Analyzer using Mg Kα radiation under a pressure of about 3 x 10^{-10} mbar. The XPS data were analyzed in XPSPeak software (version 4.1). Surface morphology was examined with a scanning electron microscope coupled with energy-dispersive X-ray spectroscopy (SEM-EDX) using Hitachi Model S-3200 N. Infrared (IR) spectra of BCs were obtained in a Bruker Platinum ATR spectrometer to analyze the surface functional groups. Mass spectra of the carbon samples were obtained using the Time-of-flight – secondary ion mass spectroscopy (ToF-SIMS) technique via a TOF SIMS V (ION TOF, Inc. Chestnut Ridge, NY) instrument. The surface profile and roughness of BCs were analyzed via a Keyence VKx1100 Confocal Laser Scanning Microscope. The pH values of the pristine biochar and all nitrogen-doped biochars were determined by recording the pH (Model: AB150 ; Manufactured by Fisher Scientific, Waltham MA, USA) of the filtrate after equilibrating 0.4 gm of BC and N-doped BC samples in 20 mL of deionized water for 24 hours at 150 rpm (El-Sayed & Bandosz, 2004). Point of zero charge (pH_{pzc}) of the samples was determined according to the previous procedure described elsewhere (Zhu & Kolar, 2014). Briefly, 0.2 gm of samples were mixed with 40 mL 0.1 N KNO_3 solution at 150 rpm for 24 hours maintained within a pH range of 2-14. The pH was adjusted by the addition of 0.1 N solution of either HNO_3 or KOH. The samples were filtered, and the pH of the filtrates was recorded. The filtrates' final pH values were then plotted against the initial pH value before the addition of BCs. The intersection point of the plotted curve with the 45° straight line ($pH_{initial} = pH_{final}$) was recorded as the sample's pH_{pzc}.

RESULTS AND DISCUSSION

A quantitative analysis of carbon and nitrogen was performed on the biochar samples. The results are shown in Table 1. All the modified samples exhibited a higher nitrogen % than BC, which indicates that nitrogen was successfully incorporated into biochar by various nitrogen-containing chemicals.. Based on the elemental analysis, MBC-400 had the highest nitrogen percentage (4.75 %) when compared to control BC (0.37 %). The samples' nitrogen content decreased with an increase in temperature, suggesting the decomposition of nitrogen moieties with low thermal stability at high temperatures (Zhou et al., 2018). Thus, the four modified samples, prepared at 400 °C, exhibited higher nitrogen content than other samples prepared at higher temperatures. Therefore, the samples prepared at 400 °C (hereafter denoted as MBC, NBC, UBC, CBC) were selected for detailed characterization, as described in the sections that follow.

Table 1: Elemental analysis (Total carbon and total nitrogen) of raw biomass, pristine and modified biochars.

Sample	Total carbon %	Total nitrogen %
Pine bark biomass	42.87	0.22
BC	69.42	0.37
NBC-400	69.46	1.79
CBC-400	68.42	2.74
UBC-400	66.02	2.59
MBC-400	64.20	4.75
NBC-500	64.68	1.55
CBC-500	67.27	1.90
UBC-500	68.72	1.29
MBC-500	69.83	1.60
NBC-600	76.89	1.04
CBC-600	75.82	1.23
UBC-600	81.07	0.75
MBC-600	81.74	1.15
NBC-700	65.90	0.69
CBC-700	77.34	0.98
UBC-700	81.09	0.66
MBC-700	80.83	1.06
NBC-800	84.14	0.67
CBC-800	79.96	0.92
UBC-800	83.60	0.53
MBC-800	83.83	0.73

The surface morphology and micro composition of the pristine and modified biochar samples were analyzed using SEM-EDX. Figure 2 depicts the SEM images (magnified at 250X). A rough surface in BC was observed whereas, MBC and CBC exhibited a smoother surface. This is due to the reaction between biochar and the corresponding nitrogen-containing chemical at elevated temperature, which resulted in a smoother surface. On the other hand, NBC and UBC have a rough morphology indicating a lesser extent of reaction with these nitrogen-containing chemicals. Consequently, the UBC and NBC possessed lower nitrogen content, which is consistent with elemental analysis. As expected, the EDX spectra (Data not shown) obtained for all the samples suggested that carbon was the principal element in all the samples. However, nitrogen was detected only in MBC. EDX analysis can probe the sample depth from 0.2 – 8 μm. The absence of nitrogen in the EDX spectra for NBC, UBC, and CBC indicates that most of the nitrogen doped in these samples was present within a few nm of the surface as explained by the XPS results later in the article.

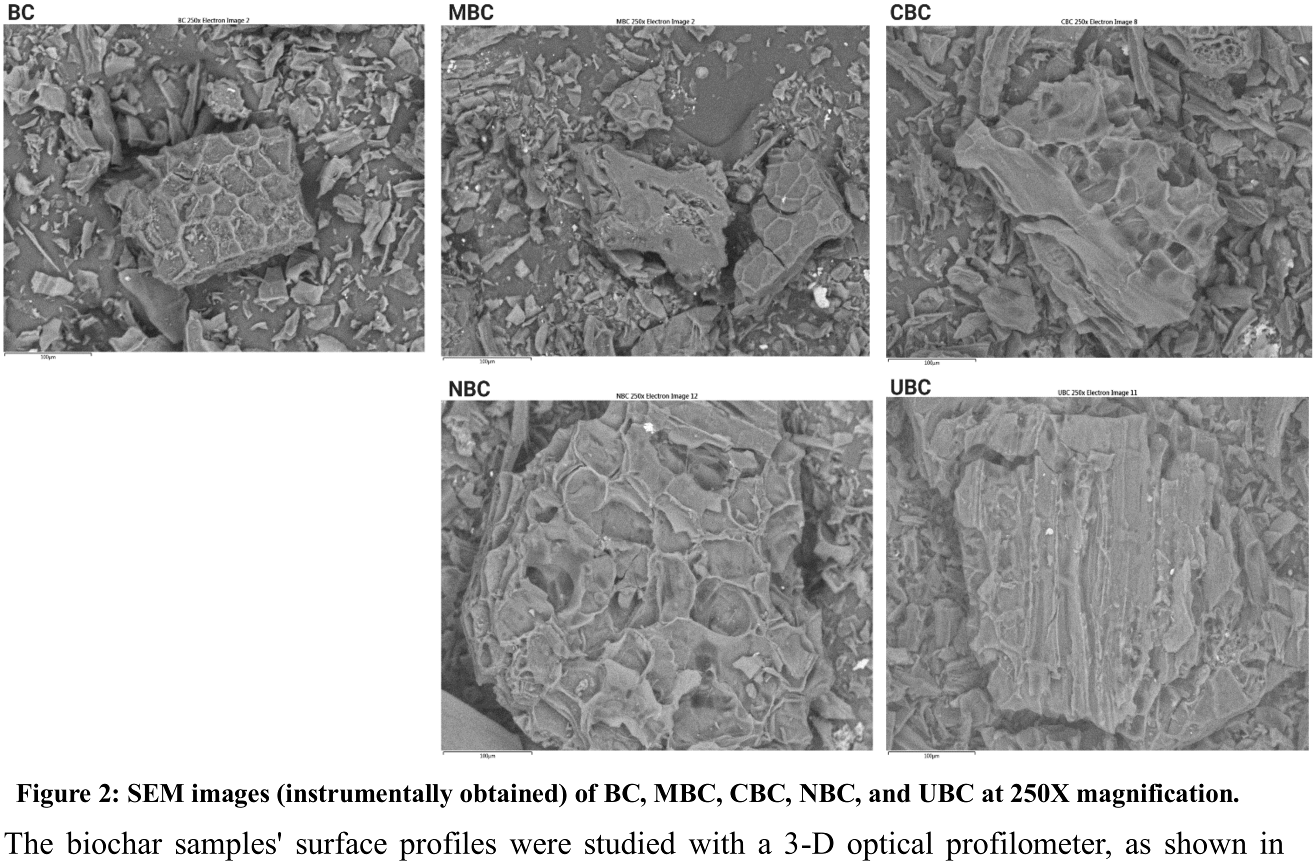

Figure 2: SEM images (instrumentally obtained) of BC, MBC, CBC, NBC, and UBC at 250X magnification.

The biochar samples' surface profiles were studied with a 3-D optical profilometer, as shown in Figure 3. The average surface roughness of BC was found to be 19.56 μm. However, after deposition, MBC, CBC, and NBC's average roughness decreased to 9.53, 13.98, and 4.02 µm, respectively. The reduction in the surface roughness of the modified samples may be attributed to the deposition of dopants on biochar's surface (Zou et al., 2011). In contrast, for UBC, mean surface roughness of 19.44 µm was recorded, indicating that urea modification did not have a considerable effect on surface roughness.

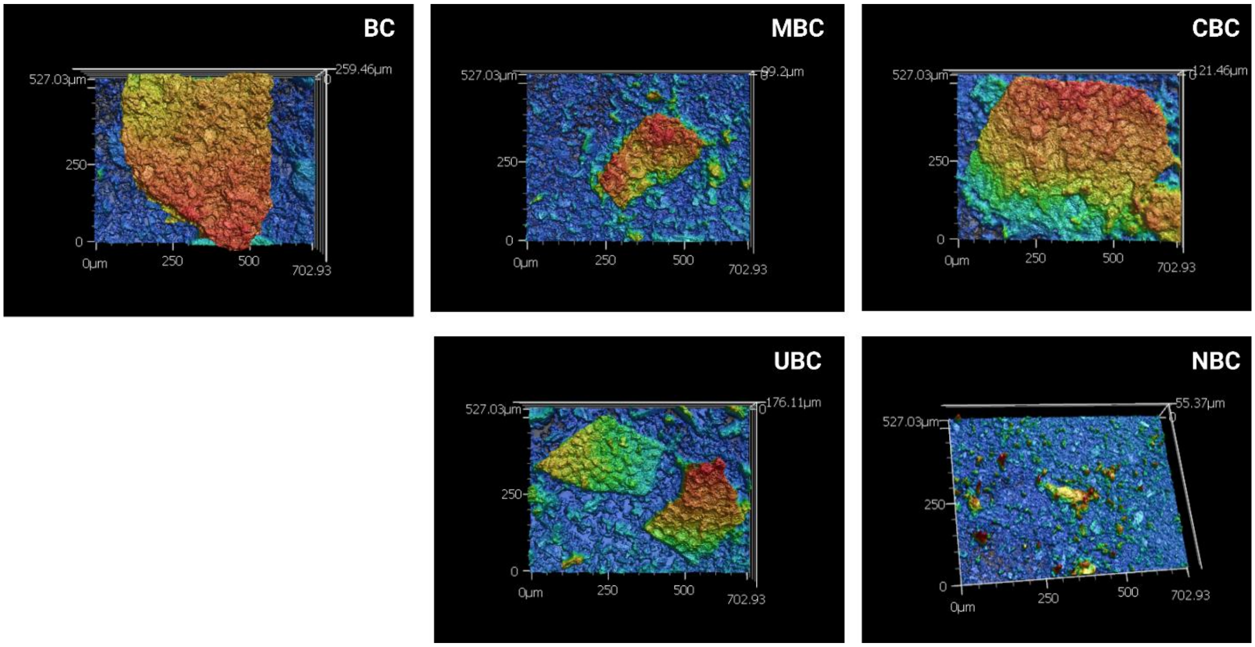

Figure 3: 3-D optical profilometer images (instrumentally obtained) of BC, MBC, CBC, NBC, and UBC.

The pH of biochar is a crucial parameter in biochars' applications in environmental, biological, and agricultural applications (Igalavithana et al., 2017). For example, high pH biochars can enhance acidic soil pH, when used as an amendment (Oni et al., 2019; Rasse et al., 2017). Moreover, biochar pH can influence the pH of the contaminant solution as well, when used as adsorbent, which will affect its pollutant remediation characteristics. Table 2 summarizes the pH values of all the biochars tested in this study. The pH value of BC was determined to be 6.5. This result was somewhat different from those reported by Khan et al. (2014), who reported a pH value of 3.0 for pine bark biochar (Khan et al., 2014). These differences may be attributed to the inherent heterogeneity of the pinewood-based feedstocks (Data shown in supplementary information: Table S1). The pH values of all the modified samples were determined to be higher than the original BC, which suggested that doping of nitrogen on the surface of biochar may have enhanced the electron lone pairs, thereby resulting in an increased surface pH compared to pristine biochar.

Table 2: The pH and pH_{pzc} of biochar samples tested in this research.

Sample	pH value	pH_{pzc}
BC	6.5	5.1
MBC	7.11	4.9
CBC	6.88	4.3
UBC	6.90	6.1
NBC	6.93	4.8

The point of zero charges (pH_{pzc}) of biochars is an essential property for employing biochars as adsorbents. It is denoted by the pH value of a solution where the biochar surface charge is neutral. If the pH value is higher than pH_{pzc}, the surface will be negatively charged and favor cationic species' adsorption. Conversely, if a solution pH is less than pH_{pzc}, the biochar surface will be positively charged and show enhanced adsorption for anionic species (Yin et al., 2019). Based on the results obtained (Table 2), the pH_{pzc} of the pristine biochar, BC was 5.1, while the nitrogen-doped biochars were found to be between 4.3 and 4.9 except for UBC, whose PZC was determined to be 6.1. These results suggested that the nitrogen-doped biochars would be suitable for removing cationic dyes at neutral pH.

The infrared spectra (400 – 4000 cm^{-1}) of pristine and modified biochars are illustrated in Figure 4. The relative difference between the transmittance of various peaks observed in the samples indicates that nitrogen modification altered biochar structure. The band range 650-850 cm^{-1} is related to aromatic structure. The signal at 1015-1315 cm^{-1} was attributed to C-N, C-C, and C-O (epoxy, hydroxyl, and carboxyl) groups. Similar observations were reported by Yin et al. (2019). The peak observed at 1576 cm^{-1} was assigned to C=O (carboxyl or lactone) groups (Yin et al., 2019). The peaks at around 1690 cm^{-1} were assigned to CH_2-CO-NH bending vibrations (X. Liu et al., 2019). The peak at 1415 cm^{-1} was ascribed to C=C bonds (Zhu & Kolar, 2014). The decrease in intensity for this bond in the modified biochar samples signifies a possible interaction between C=C groups and corresponding nitrogen-containing chemical. The incorporation of nitrogen within the carbon matrix would result in the change of electronegativity and the reactivity of the surface sites, when used in environmental and energy storage applications. C-H stretching vibration was observed at 2900 cm^{-1} in pristine biochar. However, this peak was absent from all other modified biochar samples. As complete carbonization, cannot take place at 400 °C, the disappearence of this peak might be due to reaction between C-H groups and nitrogen precursors at this temperature. The broad peak at 3200-3600 cm^{-1} was assigned to O-H stretching vibration.

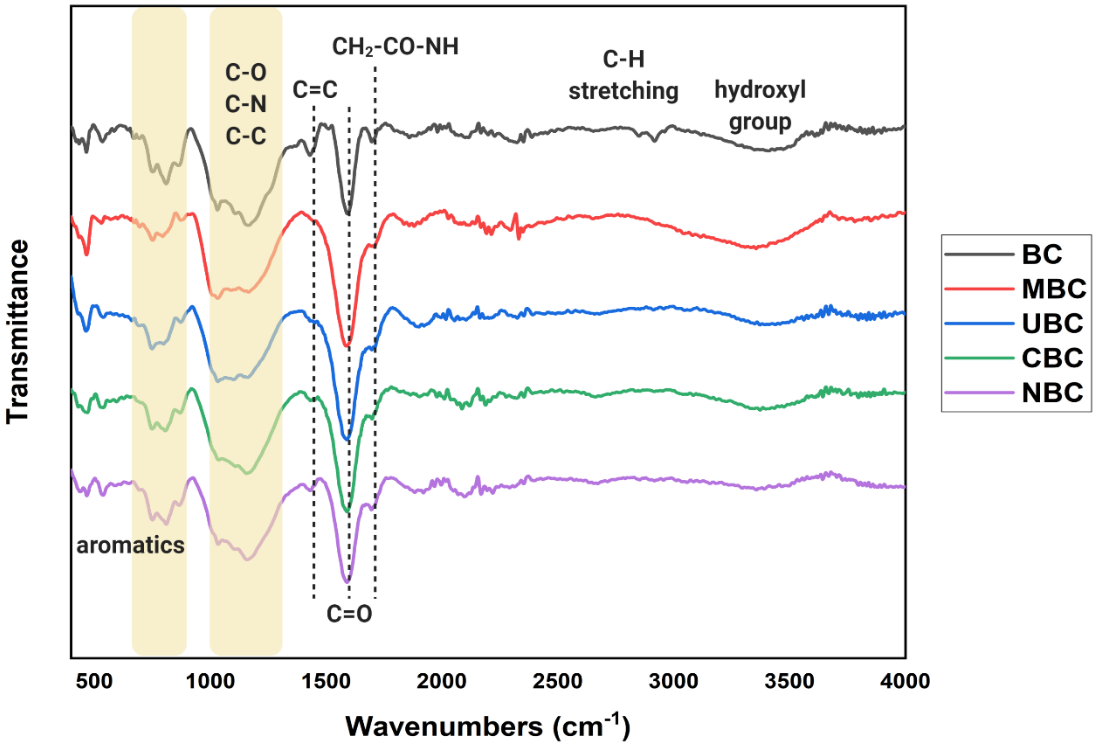

Figure 4: IR spectra of BC, MBC, CBC, NBC, and UBC.

High-resolution XPS spectra were obtained for the biochar samples to gain further information on surface functional groups. The obtained spectra were fitted with Gaussian-Lorentzian peaks with a Shirley type background. Tables 3 and 4 show the atomic compositions and relative contents of individual peaks, respectively. The MBC and CBC exhibited higher percentages of surface nitrogen than UBC and NBC, which is consistent with elemental analyses. C1s and O1s were the major peaks in all the samples (pristine and N-doped biochars) analyzed. Additionally, N1s peaks were also observed for nitrogen-modified biochar samples demonstrating successful nitrogen doping after modification. The C1s spectra were deconvoluted into three component peaks (C-1, C-2, C-3), as shown in Figure 5. C-1 represents sp^2 hybridized carbon (284.7-284.8 eV); C-2 represents C-O bonds (285.5-286.2 eV);

C-3 represents C=O (double) bonds (287-288.1 eV) (Gao et al., 2016; Yin et al., 2019).

Table 3: Atomic composition of pristine and N-doped biochar samples obtained by XPS.

Sample	C1s (%)	O1s (%)	N1s (%)
BC	86.6	13.4	-
MBC	70.9	20.8	8.3
CBC	79.9	16.2	3.9
NBC	78.5	19.2	2.3
UBC	78.2	18.2	2.9

Table 4: Relative contents of different peaks obtained by XPS spectra.

Peaks	Components	Relative content (%)				
		BC	MBC	CBC	NBC	UBC
C1s	C-1	50.08	44.38	61.57	58.78	62.68
	C-2	40.32	29.24	24.33	21.81	19.11
	C-3	9.58	26.20	13.98	29.36	18.2
O1s	O-1	6.16	16.27	16.80	24.07	23.61
	O-2	33.20	31.27	28.61	32.41	33.36
	O-3	45.37	30.13	30.28	22.30	30.49
	O-4	15.25	22.29	24.29	21.21	12.57
N1s	N-1	-	35.2	25.2	21.4	29.0
	N-2	-	13.6	23.6	23.5	18.3
	N-3	-	36.8	30.2	30.6	26.0
	N-4	-	14.2	19.6	24.2	26.6

C-1, C-2, C-3: sp^2 hybridized carbon, C-O bonds, C=O bonds respectively

O-1, O-2, O-3, O-4: carbonyl and quinone, esters, hydroxyls, and anhydrides, esters and anhydrides, carboxylic respectively

N-1, N-2, N-3, N-4: pyridinic, amine, pyrrolic, graphitic-N respectively

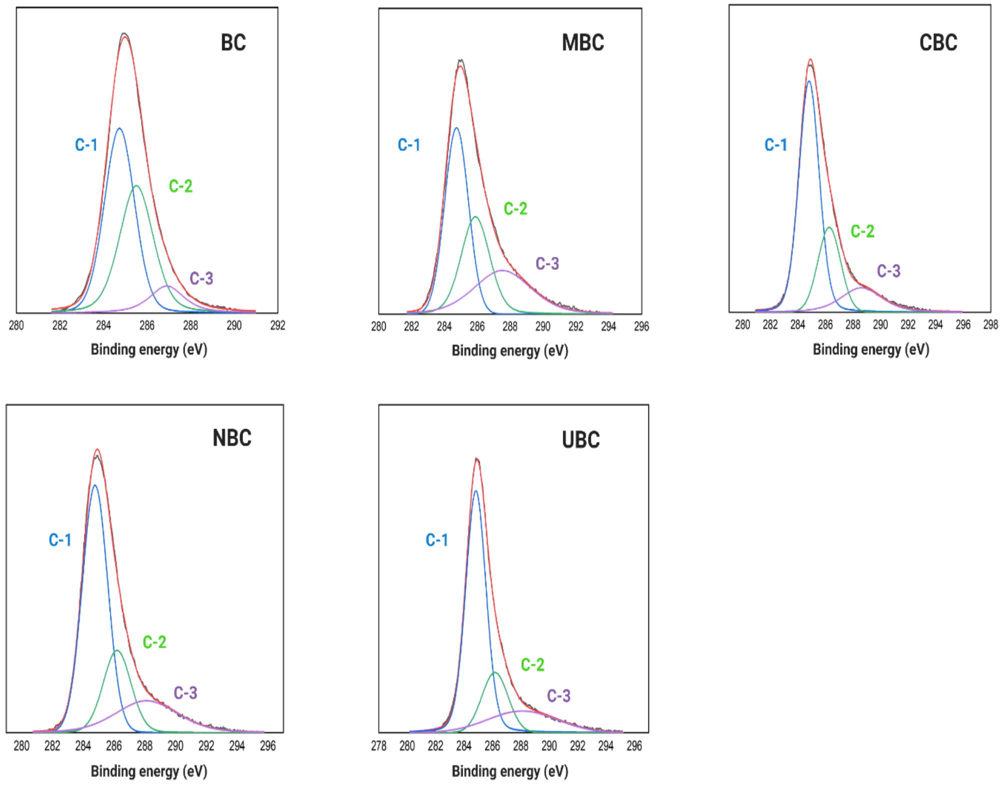

Figure 5: Deconvolution of C1s spectra for BC, MBC, CBC, NBC, and UBC. C-1: sp^2 hybridized carbon; C-2: C-O bonds; C-3: C=O bonds.

The deconvolutions of the O1s spectra for BC, MBC, CBC, NBC, and UBC are depicted in Figure 6. All O1s spectra were fitted to four components peaks (O-1, O-2, O-3, O-4). O-1 represents carbonyl and quinone (531.2-531.3 eV); O-2 represents oxygen atoms in esters, hydroxyls, and anhydrides (532.4-532.5 eV); O-3 represents ether-type oxygen atoms in esters and anhydrides (533.6-533.8 eV); O-4 represents carboxylic oxygen atoms (534.3-534.8 eV) (Chen et al., 2020). As evident from Table 4, the carbonyl oxygen content increases after N-doping, which is also consistent with the IR results.

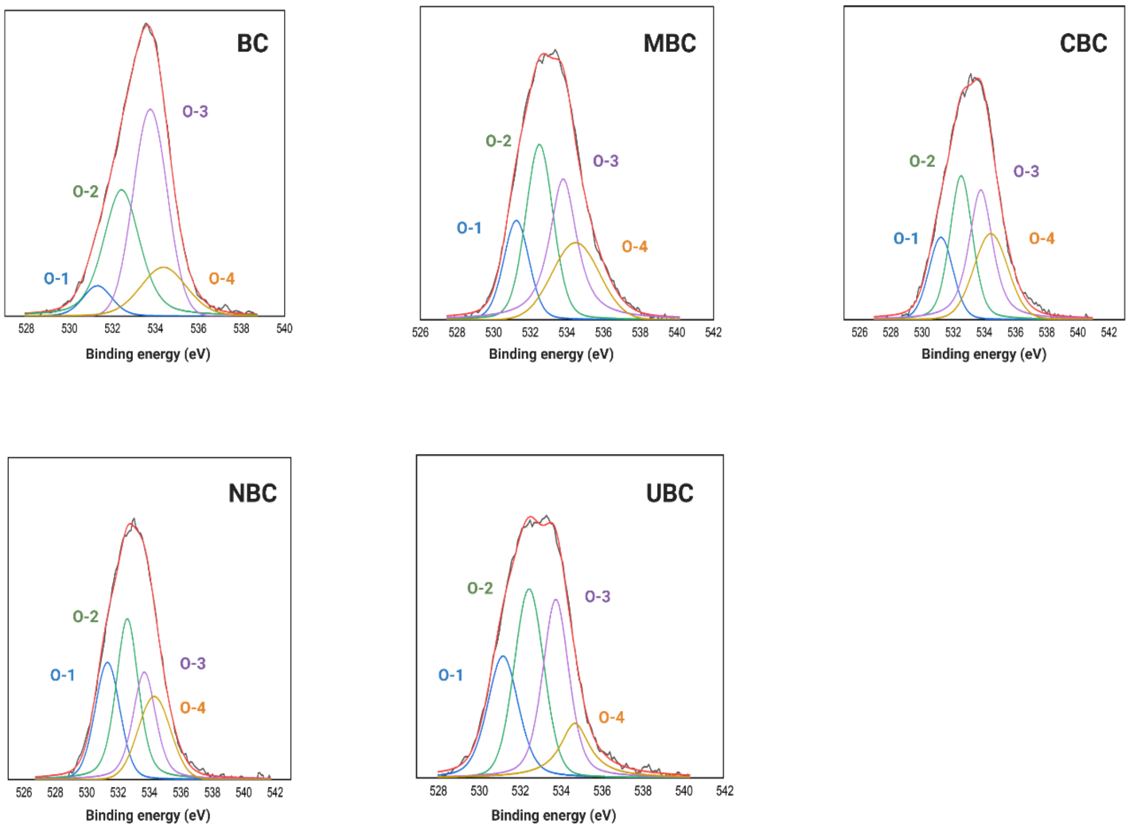

Figure 6: Deconvolution of O1s spectra for BC, MBC, CBC, NBC, and UBC. O-1: carbonyl and quinone; O-2: esters, hydroxyls, and anhydrides, O-3: esters and anhydrides, O-4: carboxylic.

The N1s spectra for all the nitrogen-modified BC samples were deconvoluted into four peaks (N-1, N-2, N-3, N-4), as shown in Figure 7. However, they differ in the location of the peaks and the intensity. N-1 represents pyridinic-N (398.5-398.7 eV); N-2 represents amine-N (399.5-399.6 eV); N-3 represents pyrrolic-N (400.3 ± 0.3 eV) and N-4 represents graphitic-N (401.4 – 401.8 eV) (Yin et al., 2019). Pyrrolic-N, and pyridinic-N, located at the graphitic layer's edges, are ring-type structures where N is bonded to two carbon atoms in a five-membered and six-membered ring, respectively (Gao et al., 2016). As seen in Table 4, MBC had a higher percentage of pyrrolic-N and pyridinic-N (36.8% and 35.2%, respectively) compared to other nitrogen-modified biochar samples, which indicates that melamine modification might favor the formation of ring-type nitrogen structures onto biochar surface. These observations are consistent with Mian et al. (2020), who reported an increase in the edge-nitrogenated pyrolysis products with an increase in melamine. On the other hand, UBC exhibited the highest percentage of graphitic-N (26.6%) compared to other N-doped biochars tested in this research. Similar observations were made by Zaeni et al. (2020), where graphitic-N increased in biochar with increasing urea: wood residue w/w ratio suggesting urea modification favored the formation of graphitic-N. Interestingly, both CBC and NBC showed similar but higher relative amounts of amine-N (23.6% and 23.5%, respectively) compared to UBC and MBC, suggesting that ammonium salts favor the formation of amine-N. Notably, CBC showed a higher percentage of elemental N than NBC, as shown in Figure 2. The reason may be attributed to the higher ammonium fraction between both the nitrogen-containing chemicals. Ammonium chloride dissociates as NH_4^+ and Cl^- in solution, and ammonium nitrate dissociates as NH_4^+ and NO_3^-. Thus, the nitrogen contribution in CBC comes from NH_4^+, whereas for NBC, it gets divided into NH_4^+ and NO_3^-. Additionally, biochars possess a negatively charged surface, which favors the electrostatic attraction with positive ammonium ion and subsequently increased N-doping.

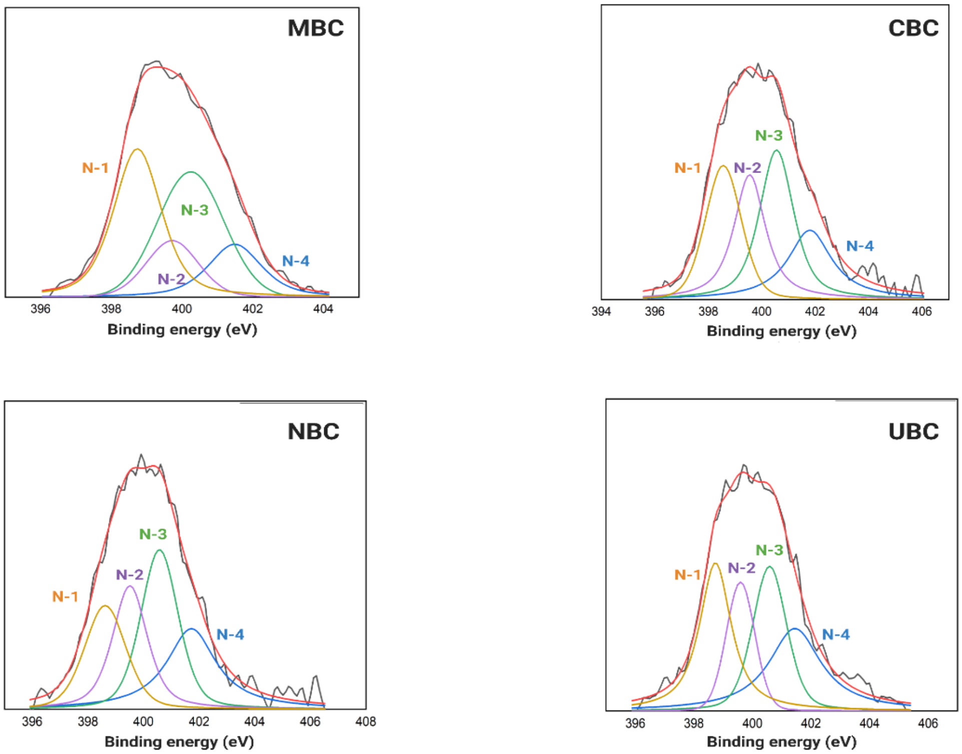

Figure 7: Deconvolution of N1s spectra for MBC, CBC, NBC, and UBC. N-1: pyridinic-N; N-2: amine-N; N-3: pyrrolic-N; N-4: graphitic-N.

Negative ion Tof-SIMS analysis of pristine and N-doped biochar samples was performed to study the interaction between BC and nitrogen nitrogen-containing chemicals. Although the intensities of the secondary ions could not be used to determine the absolute molecular compositions quantitatively as the secondary ion generation ability depends on types of solids, the relative intensity of the same ion peak across different samples can be compared to derive basic information on surface chemistry. Figure 8 shows the negative ion Tof-SIMS spectra of BC and MBC. The most intense nitrogen peaks observed in the samples are (ion, m/z value): CN^-, 26.01; CNO^-, 41.99; C_3N^-, 50.01; C_5N^-, 73.99; C_7N^-, 97.99. The intensities of these peaks increased substantially after melamine modification of the BC sample. Similar trends are also observed for other modified samples (Data not shown). The nitrogen component peaks exhibited an increase in the peak intensities. These results further validate the nitrogen enhancement in BC after modification with different N-dopants. The increase in the CNO^- peak in MBC, which could relate to amide-type structures in the samples, is consistent with XPS results. The C_6H^- peak intensity in MBC is reduced, possibly attributable to melamine interaction with C-C bonds.

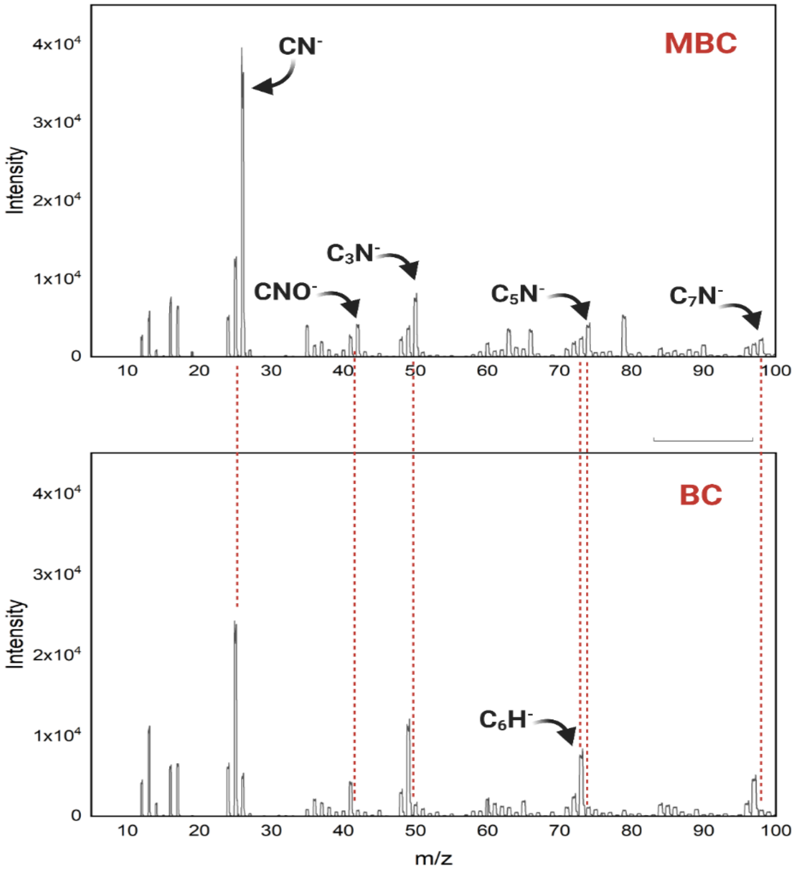

Figure 8: Negative ion Tof-SIMS spectra for BC and MBC.

In addition to Tof-SIMS spectra, high-resolution Tof-SIMS spectral images for the pristine and N-doped biochar samples were also obtained to visualize the modified biochar surfaces' distribution of nitrogen species. Original and overlaid 2D images for BC and MBC are shown in Figure 9**.** Similarly, the images for other nitrogen-doped biochars were obtained but not shown in this manuscript. TC value represents the total counts of ions, and the increase in the intensity is signified by the transition from dark red to light yellow color, as shown in figures. The overlapped images provided the distribution of elements. In this study, CN^- and C_3N^- ions were chosen to overlay on C_6H^- ion because of their high total counts compared to other species. If the ions are overlapped, a secondary color green (red + yellow) can be observed. As evident from the images, the overlapped images for BC samples had negligible, green-colored regions, whereas, for other modified samples, the green color is intensified. It can be visually analyzed from Figure 9 that MBC exhibited the maximum green intensity among all tested samples, which can be correlated to melamine interaction with biochar's carbon matrix.

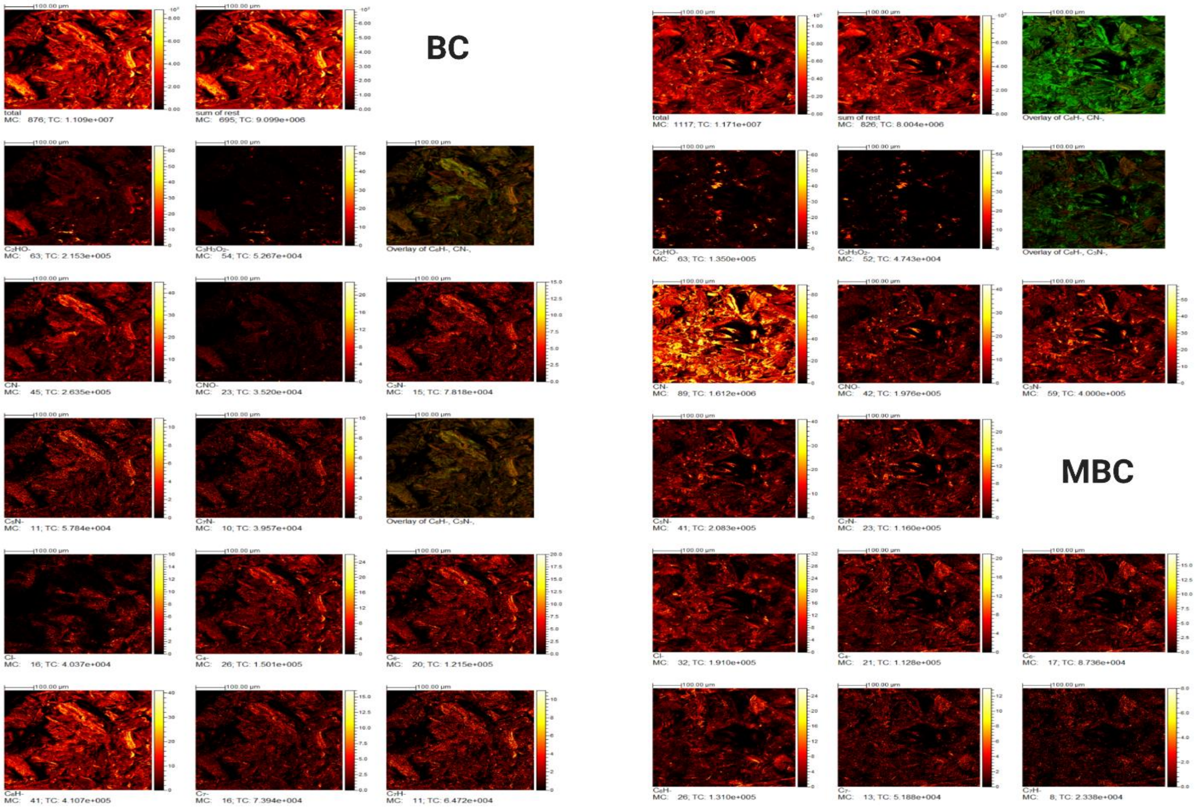

Figure 9: Tof-SIMS original and overlaid images (instrumentally obtained) of negative ions in BC and MBC. The original images are shown for all the observed ions. Overlaid images are shown for CN-, and C3N- ions on C6H- ion.

Based on the above results, it can be inferred that melamine is an efficient nitrogen-containing chemical to dope biochar with nitrogen compared to urea, ammonium chloride, and ammonium nitrate. This can be explained by the thermal stability of the different nitrogen-containing chemicals being considered. Melamine is thermally stable compared to the other three nitrogen sources. At high temperatures, it condenses to form melam with the expulsion of ammonia gas. In contrast, urea thermally degrades readily to form ammonia and carbon dioxide gas. On the other hand, both the ammonium salts degrade below 250 °C. Therefore, at high temperatures, the concentration of nitrogen available to react with the solid biochar matrix is higher when melamine is employed as a nitrogen-containing chemical, resulting in higher amounts of nitrogen in MBC.

CONCLUSIONS

In this study, we compared the surface chemistry and morphology of pine bark-derived N-doped biochars prepared with four different nitrogen-containing chemicals, namely melamine, urea, ammonium chloride, and ammonium nitrate. The results show that, under identical preparation conditions, MBC had the highest nitrogen content due to its enhanced thermal stability compared to other nitrogen-containing chemicals in the study. Pyridinic-N, pyrrolic-N, amine-N, and graphitic-N structures were present in all the nitrogen-modified samples. MBC had higher amounts of pyrrolic-N and pyridinic-N, whereas UBC had high amounts of graphitic-N. These results suggest that the structure of the nitrogen-containing chemical has a significant effect on the speciation of nitrogen on the N-doped biochars and can significantly impact their properties. More importantly, this study provides a promising approach to develop application-specific N-doped functional carbon materials from forestry wastes.

REFERENCES

Ahmad, M., Rajapaksha, A. U., Lim, J. E., Zhang, M., Bolan, N., Mohan, D., Vithanage, M., Lee, S. S., & Ok, Y. S. (2014). Biochar as a sorbent for contaminant management in soil and water: A review. In *Chemosphere* (Vol. 99, pp. 19–33). https://doi.org/10.1016/j.chemosphere.2013.10.071

Chen, W., Fang, Y., Li, K., Chen, Z., Xia, M., Gong, M., Chen, Y., Yang, H., Tu, X., & Chen, H. (2020). Bamboo wastes catalytic pyrolysis with N-doped biochar catalyst for phenols products. *Applied Energy*. https://doi.org/10.1016/j.apenergy.2019.114242

Demir, M., Ashourirad, B., Mugumya, J. H., Saraswat, S. K., El-Kaderi, H. M., & Gupta, R. B. (2018). Nitrogen and oxygen dual-doped porous carbons prepared from pea protein as electrode materials for high performance supercapacitors. *International Journal of Hydrogen Energy*. https://doi.org/10.1016/j.ijhydene.2018.03.220

Deng, J., Liu, Y., Liu, S., Zeng, G., Tan, X., Huang, B., Tang, X., Wang, S., Hua, Q., & Yan, Z. (2017). Competitive adsorption of Pb(II), Cd(II) and Cu(II) onto chitosan-pyromellitic dianhydride modified biochar. *Journal of Colloid and Interface Science*, *506*, 355–364. https://doi.org/10.1016/j.jcis.2017.07.069

El-Naggar, A., Awad, Y. M., Tang, X. Y., Liu, C., Niazi, N. K., Jien, S. H., Tsang, D. C. W., Song, H., Ok, Y. S., & Lee, S. S. (2018). Biochar influences soil carbon pools and facilitates interactions with soil: A field investigation. *Land Degradation and Development*, *29*(7), 2162–2171. https://doi.org/10.1002/ldr.2896

El-Sayed, Y., & Bandosz, T. J. (2004). Adsorption of valeric acid from aqueous solution onto activated carbons: Role of surface basic sites. *Journal of Colloid and Interface Science*, *273*(1), 64–72. https://doi.org/10.1016/j.jcis.2003.10.006

Gao, Y., Xu, S., Yue, Q., Ortaboy, S., Gao, B., & Sun, Y. (2016). Synthesis and characterization of heteroatom-enriched biochar from keratin-based and algous-based wastes. *Advanced Powder Technology*, *27*(4), 1280–1286. https://doi.org/10.1016/j.apt.2016.04.018

Igalavithana, A. D., Mandal, S., Niazi, N. K., Vithanage, M., Parikh, S. J., Mukome, F. N. D., Rizwan, M., Oleszczuk, P., Al-Wabel, M., Bolan, N., Tsang, D. C. W., Kim, K. H., & Ok, Y. S. (2017). Advances and future directions of biochar characterization methods and applications. *Critical Reviews in Environmental Science and Technology*, *47*(23), 2275–2330. https://doi.org/10.1080/10643389.2017.1421844

Khan, N., Clark, I., Sánchez-Monedero, M. A., Shea, S., Meier, S., & Bolan, N. (2014). Maturity indices in co-composting of chicken manure and sawdust with biochar. *Bioresource Technology*, *168*, 245–251. https://doi.org/10.1016/j.biortech.2014.02.123

Lehmann, J., & Joseph, S. (2012). Biochar for environmental management: Science and technology. *Biochar for Environmental Management: Science and Technology*, *1*, 1–416. https://doi.org/10.4324/9781849770552

Leng, L., Xu, S., Liu, R., Yu, T., Zhuo, X., Leng, S., Xiong, Q., & Huang, H. (2019). Nitrogen containing functional groups of biochar: An overview. *Bioresource Technology*, *298*(October 2019), 122286. https://doi.org/10.1016/j.biortech.2019.122286

Liu, F., Zuo, J., Chi, T., Wang, P., & Yang, B. (2015). Removing phosphorus from aqueous solutions by using iron-modified corn straw biochar. *Frontiers of Environmental Science and Engineering*. https://doi.org/10.1007/s11783-015-0769-y

Liu, W. J., Jiang, H., & Yu, H. Q. (2015). Development of Biochar-Based Functional Materials: Toward a Sustainable Platform Carbon Material. *Chemical Reviews*, *115*(22), 12251–12285. https://doi.org/10.1021/acs.chemrev.5b00195

Liu, W. J., Jiang, H., & Yu, H. Q. (2019). Emerging applications of biochar-based materials for energy storage and conversion. *Energy and Environmental Science*, *12*(6), 1751–1779. https://doi.org/10.1039/c9ee00206e

Liu, X., Liao, J., Song, H., Yang, Y., Guan, C., & Zhang, Z. (2019). A Biochar-Based Route for Environmentally Friendly Controlled Release of Nitrogen: Urea-Loaded Biochar and Bentonite Composite. *Scientific Reports*, *9*(1), 1–12. https://doi.org/10.1038/s41598-019-46065-3

Mian, M. M., Liu, G., & Zhou, H. (2020). Preparation of N-doped biochar from sewage sludge and melamine for peroxymonosulfate activation: N-functionality and catalytic mechanisms. *Science of the Total Environment*, *744*, 140862. https://doi.org/10.1016/j.scitotenv.2020.140862

Oni, B. A., Oziegbe, O., & Olawole, O. O. (2019). Significance of biochar application to the environment and economy. *Annals of Agricultural Sciences*, *64*(2), 222–236. https://doi.org/10.1016/j.aoas.2019.12.006

Rasse, D. P., Budai, A., O’Toole, A., Ma, X., Rumpel, C., & Abiven, S. (2017). Persistence in soil of Miscanthus biochar in laboratory and field conditions. *PLoS ONE*, *12*(9), 1–17. https://doi.org/10.1371/journal.pone.0184383

Shao, J., Zhang, J., Zhang, X., Feng, Y., Zhang, H., Zhang, S., & Chen, H. (2018). Enhance SO2 adsorption performance of biochar modified by CO2 activation and amine impregnation. *Fuel*, *224*(March), 138–146. https://doi.org/10.1016/j.fuel.2018.03.064

Wan, Z., Sun, Y., Tsang, D. C. W., Khan, E., Yip, A. C. K., Ng, Y. H., Rinklebe, J., & Ok, Y. S. (2020). Customised fabrication of nitrogen-doped biochar for environmental and energy applications. *Chemical Engineering Journal*, *401*(May). https://doi.org/10.1016/j.cej.2020.126136

Wang, J., & Wang, S. (2019). Preparation, modification and environmental application of biochar: A review. In *Journal of Cleaner Production*. https://doi.org/10.1016/j.jclepro.2019.04.282

Xiong, Z., Shihong, Z., Haiping, Y., Tao, S., Yingquan, C., & Hanping, C. (2013). Influence of NH3/CO2 Modification on the Characteristic of Biochar and the CO2 Capture. *Bioenergy Research*, *6*(4), 1147–1153. https://doi.org/10.1007/s12155-013-9304-9

Xu, Z., Li, Y., Li, D., Wang, D., Zhao, J., Wang, Z., Banis, M. N., Hu, Y., & Zhang, H. (2018). N-enriched multilayered porous carbon derived from natural casings for high-performance supercapacitors. *Applied Surface Science*. https://doi.org/10.1016/j.apsusc.2018.03.100

Yan, J., Han, L., Gao, W., Xue, S., & Chen, M. (2015). Biochar supported nanoscale zerovalent iron composite used as persulfate activator for removing trichloroethylene. In *Bioresource Technology* (Vol. 175, pp. 269–274). https://doi.org/10.1016/j.biortech.2014.10.103

Yin, W., Zhang, W., Zhao, C., & Xu, J. (2019). Evaluation of Removal Efficiency of Ni(II) and 2,4-DCP Using in Situ Nitrogen-Doped Biochar Modified with Aquatic Animal Waste. *ACS Omega*, *4*(21), 19366–19374. https://doi.org/10.1021/acsomega.9b02769

Zaeni, J. R. J., Lim, J. W., Wang, Z., Ding, D., Chua, Y. S., Ng, S. L., & Oh, W. Da. (2020). In situ nitrogen functionalization of biochar via one-pot synthesis for catalytic peroxymonosulfate activation: Characteristics and performance studies. *Separation and Purification Technology*, *241*(February), 116702. https://doi.org/10.1016/j.seppur.2020.116702

Zhang, X., Zhang, S., Yang, H., Shao, J., Chen, Y., Liao, X., Wang, X., & Chen, H. (2017). Generalized two-dimensional correlation infrared spectroscopy to reveal mechanisms of CO2 capture in nitrogen enriched biochar. *Proceedings of the Combustion Institute*, *36*(3), 3933–3940. https://doi.org/10.1016/j.proci.2016.06.062

Zhou, Q., Jiang, X., Li, X., Jia, C. Q., & Jiang, W. (2018). Preparation of high-yield N-doped biochar from nitrogen-containing phosphate and its effective adsorption for toluene. *RSC Advances*, *8*(53), 30171–30179. https://doi.org/10.1039/c8ra05714a

Zhu, Y., & Kolar, P. (2014). Adsorptive removal of p-cresol using coconut shell-activated char. *Journal of Environmental*

Chemical Engineering, *2*(4), 2050–2058. https://doi.org/10.1016/j.jece.2014.08.022

Zou, M., Beckford, S., Wei, R., Ellis, C., Hatton, G., & Miller, M. A. (2011). Effects of surface roughness and energy on ice adhesion strength. *Applied Surface Science*, *257*(8), 3786–3792. https://doi.org/10.1016/j.apsusc.2010.11.149

SUPPLEMENTARY INFORMATION

Measurement of 1g nitrogen from different nitrogen containing chemicals

Calculation for melamine:

Molar Mass of Melamine ($C_3H_6N_6$) = 126.123 g mol^{-1}

84.0402 gm Nitrogen is present in 126.123 g Melamine

Therefore, 1 gm Nitrogen is present in $\left(\frac{126.123}{84.0402} \times 1\right)$ = 1.50 g Melamine

Calculation for urea:

Molar Mass of Urea (CH_4N_2O) = 60.056 g mol^{-1}

28.0134 gm Nitrogen is present in 60.056 g Urea

Therefore, 1 gm Nitrogen is present in $\left(\frac{60.056}{28.0134} \times 1\right)$ = 2.14 g Urea

Calculation for ammonium chloride:

Molar Mass of Ammonium Chloride (ClH_4N) = 53.49 g mol^{-1}

14.0067 gm Nitrogen is present in 53.49 g Ammonium Chloride

Therefore, 1 gm Nitrogen is present in $\left(\frac{53.49}{14.0067} \times 1\right)$ = 3.82 g Ammonium Chloride

Calculation for ammonium nitrate:

Molar Mass of Ammonium Nitrate (NH_4NO_3) = 80.043 g mol^{-1}

28.0134 gm Nitrogen is present in 80.043 g Ammonium Nitrate

Therefore, 1 gm Nitrogen is present in $\left(\frac{80.043}{28.0134} \times 1\right)$ = 2.85 g Ammonium Nitrate

Table S1: Pinewood-based feedstock characteristics

Feedstock	C %	N %	S %	Reference
Pine sawdust	49.77	0.06	0.01	Khan et al. (2013)
Pinebark nuggets	42.87	0.22	0.03	This work